

# Generalized matrix method for calculation of internal light energy flux in mixed coherent and incoherent multilayers

Emanuele Centurioni

A generalized matrix method to treat multilayer systems with mixed coherent and incoherent optical behavior is presented. The method is based on the calculation of the light energy flux inside the multilayer, whose internal light absorption is straightforwardly derived. The Poynting vector is used to derive the light energy flux in the case of a layer with coherent behavior. Multilayer structures with any distribution of layers with coherent or incoherent behavior can be treated, including the case of oblique incidence. Use of the light energy flux instead of the more commonly used light intensity permits the calculation of light absorption with a better accuracy and a much shorter computation time. © 2005 Optical Society of America

OCIS codes: 200.4860, 230.4170, 300.1030.

## 1. Introduction

To simulate experimental spectral measurements of a multilayer system it is usually necessary to treat some layers as coherent (internal interference taken into account) and others as incoherent (internal interference ignored). This is true, for instance, when a thin layer is deposited on top of a glass. Because the glass is very thick (compared with the radiation wavelength) and transparent, we should treat it as incoherent. If we do not, we have multiple reflections that lead to narrow oscillations in the calculated reflectance and transmittance spectra that are not present in the experimental data. Interference-destroying causes are the limited resolution of the instrument, the nonperfectly parallel glass surfaces, and the limited light source coherence length.<sup>1-3</sup> The simulation of an optical quantity like total transmittance ( $T$ ), reflectance ( $R$ ), and internal light absorption ( $A$ ) is commonly used in many fields, as in optical coating design, solar cell optimization, thin-film measurement systems, interferometric infrared absorber and emitter design, analysis of various spectroscopic methods, etc.

From the scattering-matrix formalism for a coherent multilayer,<sup>4</sup> several attempts were made to define a formalism able to include incoherent layers as well<sup>1,5,3</sup> and with the possibility of calculating the internal light absorption.<sup>5-8</sup> Some authors<sup>6,7</sup> computed the internal light absorption  $A$  of the thickness from depth  $z_1$  to depth  $z_2$  by means of integration of the light intensity  $I$ :

$$A_{z_1 \leq z \leq z_2} = \int_{z_1}^{z_2} \alpha(z) I(z) dz, \quad (1)$$

where the light intensity is a function of the electric field  $I(z) = f_1[\mathbf{E}(z), \dots]$  and  $\alpha$  is the absorption coefficient.

Other authors<sup>5,8</sup> solved the problem in a more elegant way: They computed the light energy flux  $\Phi$  so that the light absorption is simply given by

$$A_{z_1 \leq z \leq z_2} = \Phi(z_1) - \Phi(z_2), \quad (2)$$

where  $\Phi(z) = f_2[\mathbf{E}(z), \dots]$ . When the layer is coherent, the Poynting vector is used to compute  $\Phi$ . This second approach has two advantages over the first one: It is more accurate because there is no approximation that is due to discretization (the first approach requires an integration) and the computer algorithm is simplified, resulting in a shorter execution time.

The author (centurioni@bo.imm.cnr.it) is with the Consiglio Nazionale delle Ricerche, Istituto per la Microelettronica e Microsistemi, Via P. Gobetti 101, I-40129 Bologna, Italy.

Received 6 July 2005; accepted 29 July 2005.

0003-6935/05/357532-08\$15.00/0

© 2005 Optical Society of America

So far the case of oblique incidence has been covered in the literature for only the first approach.

In this work I present a generalized matrix method to treat mixed coherent–incoherent multilayers based on the second approach. The method is able to calculate the total transmittance, reflectance, internal light energy flux, and internal light energy absorption, including the case of oblique incidence. Finally, I give an example of the application of the present method in the analysis of typical amorphous-silicon pin solar cells.

## 2. Theory

### A. Coherent Multilayers

Let us assume a multilayer structure with  $m$  isotropic and homogeneous layers and plane and parallel interfaces (see Fig. 1). A positive direction is assigned to the light moving from left to right. The semi-infinite media on the left (0) and on the right ( $m + 1$ ) are the ambient media (usually air). Light passing through this structure can be described with the scattering-matrix formalism<sup>4</sup>:

$$\begin{bmatrix} E_{0R}^+ \\ E_{0R}^- \end{bmatrix} = \mathbf{S} \begin{bmatrix} E_{(m+1)L}^+ \\ E_{(m+1)L}^- \end{bmatrix}, \quad (3)$$

where  $E_{0R}$  is the electric field just before the first interface,  $E_{0R}^+$  is associated with the wave propagating in the positive direction and  $E_{0R}^-$  is that in the negative direction,  $E_{(m+1)L}$  is the electric field just after the last interface, and  $\mathbf{S}$  is the  $2 \times 2$  scattering matrix,

$$\mathbf{S} = \mathbf{I}_{01} \mathbf{L}_1 \mathbf{I}_{12} \cdots \mathbf{L}_m \mathbf{I}_{(m+1)}, \quad (4)$$

where  $\mathbf{I}_{j(j+1)}$  defines the wave propagation at the interface between the film  $j$  and  $j + 1$  and  $\mathbf{L}_j$  describes the wave propagation through the film  $j$ .

The matrix  $\mathbf{I}$  is defined as

$$\mathbf{I}_{i,j} = \frac{1}{t_{ij}} \begin{bmatrix} 1 & r_{ij} \\ r_{ij} & 1 \end{bmatrix}, \quad (5)$$

where  $t_{ij}$  and  $r_{ij}$  are the Fresnel coefficients at the interface  $ij$ :

$$r_{ij,p} = \frac{N_j \cos \phi_i - N_i \cos \phi_j}{N_j \cos \phi_i + N_i \cos \phi_j}, \quad (6)$$

$$r_{ij,s} = \frac{N_i \cos \phi_i - N_j \cos \phi_j}{N_i \cos \phi_i + N_j \cos \phi_j}, \quad (7)$$

$$t_{ij,p} = \frac{2N_i \cos \phi_i}{N_j \cos \phi_i + N_i \cos \phi_j}, \quad (8)$$

$$t_{ij,s} = \frac{2N_i \cos \phi_i}{N_i \cos \phi_i + N_j \cos \phi_j}, \quad (9)$$

where  $N$  is the complex index of refraction of the

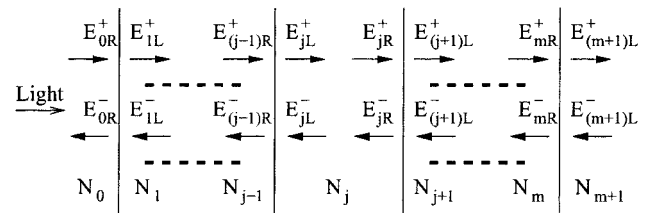


Fig. 1. Schematic representation of a multilayer with forward- and backward-propagating electric field components shown.

material ( $N = n + ik$ ),  $\phi$  is the complex propagation angle ( $\phi = 0$  for light perpendicular to the interfaces) following Snell's law ( $N_0 \sin \phi_0 = N_1 \sin \phi_1 = \cdots = N_{m+1} \sin \phi_{m+1}$ ), and the suffixes  $p$  and  $s$  refer to the wave polarization state parallel ( $p$  polarized or TM waves) and perpendicular ( $s$  polarized or TE waves) to the incident plane, respectively.

The matrix  $\mathbf{L}$  is defined as

$$\mathbf{L}_j = \mathbf{L}(\beta_j) = \begin{bmatrix} \exp(-i\beta_j) & 0 \\ 0 & \exp(i\beta_j) \end{bmatrix}, \quad (10)$$

where  $\beta$  is the phase shift that is due to the wave passing through the film  $j$  and is defined by the equation

$$\beta_j = \frac{2\pi d_j N}{\lambda} \cos \phi_j, \quad (11)$$

where  $\lambda$  is the wavelength of the incident light and  $d$  is the layer thickness.

From the scattering matrix it is possible to calculate the front-reflectance and front-transmittance coefficients,

$$r = \frac{E_{0R}^-}{E_{0R}^+} = \frac{S_{21}}{S_{11}}, \quad (12)$$

$$t = \frac{E_{(m+1)L}^+}{E_{0R}^+} = \frac{1}{S_{11}}, \quad (13)$$

and the back-reflectance and back-transmittance coefficients,

$$r' = \frac{E_{(m+1)L}^-}{E_{(m+1)L}^+} = -\frac{S_{12}}{S_{11}}, \quad (14)$$

$$t' = \frac{E_{0R}^-}{E_{(m+1)L}^-} = \frac{\det \mathbf{S}}{S_{11}}. \quad (15)$$

By use of the complex Poynting vector definition<sup>9,10</sup> [see Eqs. (48) and (49)] it can be demonstrated that the light energy flux (normal to the interfaces) associated with a single wave moving forward or backward is given by

$$\Phi = C|E_s|^2 \operatorname{Re}(N \cos \phi), \quad (16)$$

$$\Phi = C|E_p|^2 \operatorname{Re}(N^* \cos \phi), \quad (17)$$

for  $s$  and  $p$  polarization, respectively, where  $C$  is a constant,  $\operatorname{Re}$  indicates the real part of  $N$ , and  $N^*$  is the complex conjugate of  $N$ . Equations (16) and (17) can be applied to the semi-infinite medium on the right-hand side of Fig. 1 [there is only one transmitted wave, i.e.,  $E_{(m+1)L}^- = 0$ ] but cannot be applied to the semi-infinite medium on the left-hand side (there are two waves, the incident wave and the reflected wave). Fortunately in the special case of a transparent medium (real  $N_0$ ) it is possible to treat incident and reflected light as separate beams. Because there is no wave attenuation ( $|E|$  has no spatial dependencies), one can imagine computing Eqs. (16) and (17) far away from the surface where the interference contribution is negligible.

If  $N_0$  is real, from Eqs. (12)–(17) we have that the energy reflectivity is

$$R = |r|^2 \quad (18)$$

for both polarizations, and the energy transmittances are

$$T_s = \frac{|t_s|^2 \operatorname{Re}(N_{m+1} \cos \phi_{m+1})}{N_0 \cos \phi_0}, \quad (19)$$

$$T_p = \frac{|t_p|^2 \operatorname{Re}(N_{m+1}^* \cos \phi_{m+1})}{N_0 \cos \phi_0}. \quad (20)$$

Note that in the case of unpolarized light  $R$  and  $T$  can be simply computed as

$$R = \frac{R_p + R_s}{2},$$

$$T = \frac{T_p + T_s}{2} \quad (21)$$

### B. Incoherent Multilayers

In the case of a multilayer structure of incoherent layers, a matrix formalism similar to the case of coherent layers can be used.<sup>2,3</sup> If we substitute the electric field  $E$  with its amplitude square  $U = |E|^2$  (see Fig. 2), Eqs. (3), (4), and (11)–(15) are still valid.

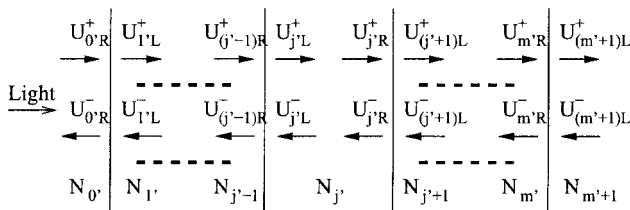


Fig. 2. Schematic representation of a multilayer with  $U = |E|^2$  forward- and backward-propagating components shown.

Equation (3) becomes

$$\begin{bmatrix} U_{0R}^+ \\ U_{0R}^- \end{bmatrix} = \bar{\mathbf{S}} \begin{bmatrix} U_{(m+1)L}^+ \\ U_{(m+1)L}^- \end{bmatrix}, \quad (22)$$

where we use  $\bar{\mathbf{S}}$  instead of  $\mathbf{S}$  to distinguish between the incoherent and the coherent case. Equation (4) becomes

$$\bar{\mathbf{S}} = \bar{\mathbf{I}}_{0'1} \bar{\mathbf{L}}_{1'} \bar{\mathbf{I}}_{1'2'} \dots \bar{\mathbf{L}}_{m'} \bar{\mathbf{I}}_{m'(m'+1)}, \quad (23)$$

where again  $\bar{\mathbf{I}}_{j'(j'+1)}$  defines the wave propagation at the interface between the film  $j'$  and  $j' + 1$  and  $\bar{\mathbf{L}}_{j'}$  describes the wave propagation through the film  $j'$ .

The matrix  $\bar{\mathbf{I}}$  can be defined as

$$\bar{\mathbf{I}}_{j'(j'+1)} = \frac{1}{|t|^2} \begin{bmatrix} 1 & -|r'|^2 \\ |r|^2 & |tt'|^2 - |rr'|^2 \end{bmatrix}, \quad (24)$$

where  $r$  and  $t$  are the complex reflection and transmission coefficients, respectively, of the interface  $j'(j' + 1)$  for light moving in a positive direction and  $r'$  and  $t'$  are for light moving in a negative direction:

$$r = \frac{E_{j'R}^-}{E_{j'R}^+}, \quad t = \frac{E_{(j'+1)L}^+}{E_{j'R}^+}, \quad (25)$$

$$r' = \frac{E_{(j'+1)L}^+}{E_{(j'+1)L}^-}, \quad t' = \frac{E_{j'R}^-}{E_{(j'+1)L}^-}. \quad (26)$$

Of course the matrix  $\bar{\mathbf{I}}$  can also be calculated from the indices of refraction of the two films bonding the interface. However, as will be clear later, Eq. (24) is actually all we need.

The matrix  $\bar{\mathbf{L}}$  is defined as

$$\bar{\mathbf{L}}_{j'} = \bar{\mathbf{L}}(\beta_{j'}) = \begin{bmatrix} |\exp(-i\beta_{j'})|^2 & 0 \\ 0 & |\exp(i\beta_{j'})|^2 \end{bmatrix}. \quad (27)$$

Equations (12), (13), (14), and (15) become, respectively,

$$\bar{r} = \frac{U_{0R}^-}{U_{0R}^+} = \frac{\bar{S}_{21}}{\bar{S}_{11}}, \quad (28)$$

$$\bar{t} = \frac{U_{(m+1)L}^+}{U_{0R}^+} = \frac{1}{\bar{S}_{11}}, \quad (29)$$

$$\bar{r}' = \frac{U_{(m+1)L}^+}{U_{(m+1)L}^-} = -\frac{\bar{S}_{12}}{\bar{S}_{11}}, \quad (30)$$

$$\bar{t}' = \frac{U_{0R}^-}{U_{(m+1)L}^-} = \frac{\det \bar{\mathbf{S}}}{\bar{S}_{11}}. \quad (31)$$

If light is incident from the left-hand side and the semi-infinite medium on that side is transparent ( $N_{0'}$  is real), then the total energy reflectivity is

$$R = \bar{r} \quad (32)$$

for both polarizations, and the transmittances are

$$T_s = \frac{\bar{t}_s \operatorname{Re}(N_{m'+1} \cos \phi_{m'+1})}{N_{0'} \cos \phi_{0'}}, \quad (33)$$

$$T_p = \frac{\bar{t}_p \operatorname{Re}(N_{m'+1}^* \cos \phi_{m'+1})}{N_{0'} \cos \phi_{0'}}, \quad (34)$$

for  $s$  and  $p$  polarization, respectively. Note that, whereas  $\mathbf{S}$  is complex,  $\bar{\mathbf{S}}$  is real.

At this point we cannot compute  $R$  and  $T$  because we still need to explicate the interface matrices  $\bar{\mathbf{I}}$ . This is done in the next subsection.

### C. Mixed Coherent and Incoherent Multilayers

In the case of a multilayer structure with some of the layers to be treated as coherent and others as incoherent, the following formalism can be used.<sup>1,3</sup> The multilayer can be ideally divided into incoherent layers and packets of coherent layers (see Fig. 3). For each packet of coherent layers the classical formalism can be used to find the associated scattering matrix  $\mathbf{S}$  and therefore the associated  $r$ ,  $t$  and  $r'$ ,  $t'$  values. These values can be used to calculate an equivalent incoherent interface  $\bar{\mathbf{I}}$ , as suggested by Eq. (24), reducing the mixed coherent–incoherent problem to the incoherent case. Note that even the case of a single interface separating two incoherent layers can be treated with the same formalism.

Let us assume a packet of  $m$  coherent layers, as in Fig. 1, to be part of a mixed coherent–incoherent multilayer, as in Fig. 3, where the layers 0 and  $m + 1$  of Fig. 1 correspond to the layers  $i'$  and  $i' + 1$  of Fig. 3, respectively. From Eqs. (12)–(15) and (24) we have

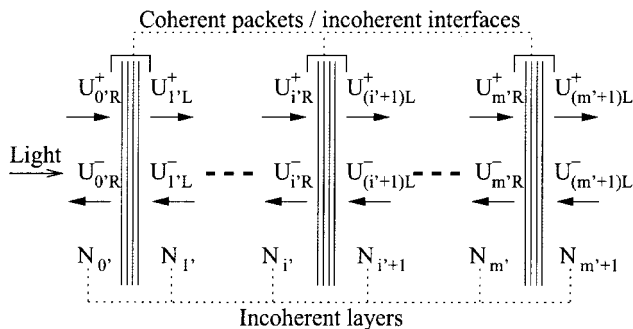


Fig. 3. Schematic representation of a mixed coherent–incoherent multilayer structure with  $U = |E|^2$  forward- and backward-propagating components shown.

$$\bar{\mathbf{I}}_{i'(i'+1)} = \begin{bmatrix} |S_{11}|^2 & -|S_{12}|^2 \\ |S_{21}|^2 & \frac{|\det \mathbf{S}|^2 - |S_{12}S_{21}|^2}{|S_{11}|^2} \end{bmatrix}. \quad (35)$$

By use of Eq. (35), every coherent packet or simple interface can be converted into the corresponding incoherent interface  $\bar{\mathbf{I}}$ , and  $\bar{\mathbf{S}}$ ,  $R$ , and  $T$  can be finally computed.

### D. Light Energy Flux in Incoherent Layers in a Mixed Coherent–Incoherent Multilayer

$U$  inside the incoherent layer  $i'$  just before the interface  $i'(i' + 1)$  (see Fig. 3) can be computed as

$$\begin{bmatrix} U_{i'R}^+ \\ U_{i'R}^- \end{bmatrix} = \bar{\mathbf{S}}_{i'} \begin{bmatrix} U_{(m'+1)L}^+ \\ U_{(m'+1)L}^- \end{bmatrix}, \quad (36)$$

where

$$\bar{\mathbf{S}}_{i'} = \bar{\mathbf{I}}_{i'(i'+1)} \bar{\mathbf{L}}_{i'+1} \cdots \bar{\mathbf{L}}_m \bar{\mathbf{I}}_{m'(m'+1)}. \quad (37)$$

Using Eq. (29) and considering that  $U_{(m'+1)L}^- = 0$  (on the right-hand side there is only the transmitted wave), we have

$$\begin{bmatrix} U_{i'R}^+ \\ U_{i'R}^- \end{bmatrix} = \bar{\mathbf{S}}_{i'} \begin{bmatrix} 1 \\ \bar{S}_{11} \\ 0 \end{bmatrix} U_{i'R}^+. \quad (38)$$

Because the layer is incoherent, forward and backward light beams do not interfere with each other and can be treated separately as a single beam, so from Eqs. (16) and (17) we have that the corresponding light energy flux  $\Phi$  is

$$\begin{bmatrix} \Phi_{i'R}^+ \\ \Phi_{i'R}^- \end{bmatrix} = \bar{\mathbf{S}}_{i'} \begin{bmatrix} 1 \\ \bar{S}_{11} \\ 0 \end{bmatrix} \gamma \Phi_{0'R}^+, \quad (39)$$

where  $\Phi_{0'R}^+$  is the incident energy flux and  $\gamma$ , if  $N_{0'}$  is real, is given by

$$\gamma_s = \frac{\operatorname{Re}(N_{i'} \cos \phi_{i'})}{N_{0'} \cos \phi_{0'}}, \quad \gamma_p = \frac{\operatorname{Re}(N_{i'}^* \cos \phi_{i'})}{N_{0'} \cos \phi_{0'}} \quad (40)$$

for  $s$  and  $p$  polarization, respectively.

The  $\Phi$  profile inside layer  $i$  can be computed as

$$\begin{bmatrix} \Phi_{i'}^+(z) \\ \Phi_{i'}^-(z) \end{bmatrix} = \bar{\mathbf{L}} \left( \beta_{i'} \frac{d_{i'} - z}{d_{i'}} \right) \begin{bmatrix} \Phi_{i'R}^+ \\ \Phi_{i'R}^- \end{bmatrix}, \quad (41)$$

where  $z$  is measured from the interface  $(i' - 1)i'$ . If we assign to  $\Phi_{0'R}^+$  unit value, Eq. (41) directly gives the energy flux (forward and backward) normalized to the incident energy flux.

The net energy flux (normalized to the incident

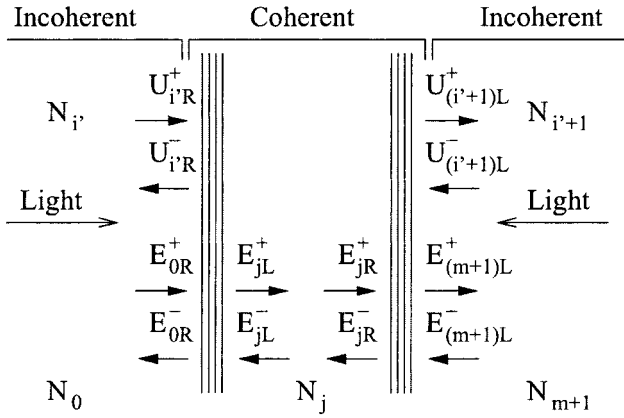


Fig. 4. Detail of a mixed coherent-incoherent multilayer structure with  $U = |E|^2$  and  $E$  forward- and backward-propagating components shown.

energy flux) is, of course,

$$\Phi_{i'}(z) = \Phi_{i'}^+(z) - \Phi_{i'}^-(z). \quad (42)$$

#### E. Light Energy Flux in Coherent Layers in a Mixed Coherent-Incoherent Multilayer

Let us consider a packet of coherent multilayers embedded in a mixed coherent-incoherent structure, as shown in Fig. 4. We observe that the coherent packet sees an incoherent light flux coming from the left-hand side with an associated electric field intensity defined by  $(U_{i'R}^+)^{1/2}$  and an incoherent light flux coming from the right-hand side with an associated electric field intensity defined by  $[U_{(i'+1)L}^-]^{1/2}$ . There is no coherence between the two fluxes, so the problem can be separated by use of the superposition principle and can be reduced to the case of a simple coherent multilayer, with light coming from the left- or from the right-hand side.

We consider first light flux coming from the left-hand side. Based on similar considerations, equations like Eq. (38) can also be written for the electric field inside the layer  $j$ :

$$\begin{bmatrix} E_{jR}^+ \\ E_{jR}^- \end{bmatrix} = \mathbf{S}_j \begin{bmatrix} E_{(m+1)L}^+ \\ 0 \end{bmatrix} = \mathbf{S}_j \begin{bmatrix} 1 \\ S_{11} \\ 0 \end{bmatrix} E_{0R}^+, \quad (43)$$

where

$$\mathbf{S}_j = \mathbf{I}_{j(j+1)} \mathbf{L}_{j+1} \cdots \mathbf{L}_m \mathbf{I}_{m(m+1)}. \quad (44)$$

We can link the electric field to the light flux coming from the left-hand side as follows:

$$\frac{E_{0R}^+}{E_{0R}^+} = \left( \frac{U_{i'R}^+}{U_{0R}^+} \right)^{1/2}. \quad (45)$$

Finally, using Eqs. (45) and (38), we have

$$E_{0R}^+ = \left\{ (1, 0) \bar{\mathbf{S}}_{i'} \begin{bmatrix} 1 \\ \bar{S}_{11} \\ 0 \end{bmatrix} \right\}^{1/2} E_{0R}^+, \quad (46)$$

where  $E_{0R}^+$  is the electric field intensity just on the left-hand side of the first layer of the whole multilayer. The electric field profile in layer  $j$  can be expressed as

$$\begin{bmatrix} E_j^+(z) \\ E_j^-(z) \end{bmatrix} = \mathbf{L} \left( \beta_j \frac{d_j - z}{d_j} \right) \begin{bmatrix} E_{jR}^+ \\ E_{jR}^- \end{bmatrix}, \quad (47)$$

where  $z$  is measured from the interface  $(j-1)j$ . Once the electric field profile is known, it is possible to compute the energy flux by use of the complex Poynting vector.<sup>9,10</sup> If  $N_{0'}$  is real and we set  $E_{0R}^+ = 1$ , the normalized Poynting vector  $\langle \mathbf{S} \rangle$ , giving the energy flux along the direction of propagation, can be defined as

$$\langle \mathbf{S} \rangle(z) = c \frac{\text{Re}\{\mathbf{E}(z) \times [\mathbf{B}(z)]^*\}}{N_{0'} \cos \phi_{0'}}, \quad (48)$$

where  $c$  is the speed of light and  $\mathbf{B}$  is the magnetic field. What we actually need is the  $z$  component (assuming that  $z$  is perpendicular to the multilayer surface) of such a vector:

$$\Phi(z) = \langle \mathbf{S} \rangle(z) \cdot [0, 0, 1]. \quad (49)$$

Of course, when Eq. (49) is used, the resulting energy flux of the impinging light (with  $E_{0R}^+ = 1$ ) has unit value. To compute the cross product between vectors it is convenient to explicate each component in  $x$ ,  $y$ , and  $z$ . Assuming that the plane containing the wave is on  $yz$ , for  $s$ -polarized light we have

$$\mathbf{E}_f(z) = [1, 0, 0] E_j^+(z), \quad (50)$$

$$\mathbf{E}_b(z) = [1, 0, 0] E_j^-(z), \quad (51)$$

for light moving in the positive direction and the negative direction, respectively. In the case of  $p$ -polarized light we have

$$\mathbf{E}_f(z) = [0, \cos \phi, -\sin \phi] E_j^+(z), \quad (52)$$

$$\mathbf{E}_b(z) = [0, -\cos \phi, -\sin \phi] E_j^-(z). \quad (53)$$

Note that in Eqs. (52) and (53) we used the Verdet convention because the Fresnel convention is not appropriate with our choice of coordinate system.<sup>11</sup>

For  $\mathbf{E}(z)$  we have

$$\mathbf{E}(z) = \mathbf{E}_f(z) + \mathbf{E}_b(z). \quad (54)$$

The magnetic field  $\mathbf{B}(z)$  that accompanies this electric field can be derived from Maxwell's equations:

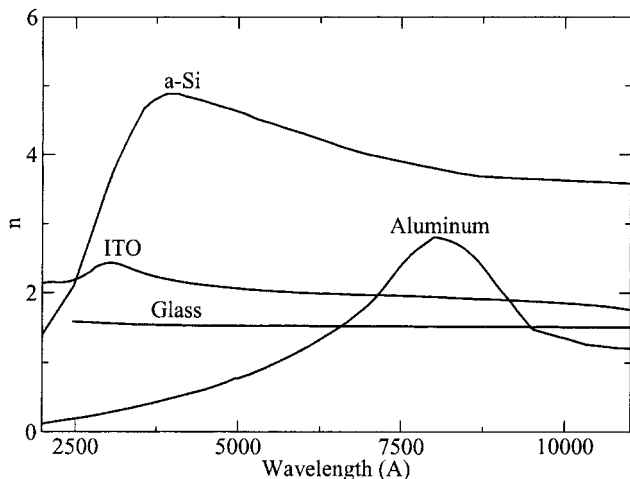


Fig. 5. Refractive index spectra used for the simulations.

$$\mathbf{B}(z) = \frac{N_j \mathbf{u}_f \times \mathbf{E}_f(z) + N_j \mathbf{u}_b \times \mathbf{E}_b(z)}{c}, \quad (55)$$

where  $\mathbf{u}$  is the complex unit vector defining the direction of wave propagation:

$$\mathbf{u}_f = [0, \sin \phi, \cos \phi], \quad \mathbf{u}_b = [0, \sin \phi, -\cos \phi]. \quad (56)$$

With Eq. (49) it is now possible to compute the contribution to the energy flux for light coming from the left-hand side,  $\Phi_j^l(x)$ .

We now consider a light flux coming from the right-hand side. Using Eq. (14) and considering that both  $E_{(m+1)L}^+$  and  $E_{(m+1)L}^-$  are nonzero because we have both incident and reflected waves, we have

$$\begin{bmatrix} E_{jR}^+ \\ E_{jR}^- \end{bmatrix} = \mathbf{S}_j \begin{bmatrix} E_{(m+1)L}^+ \\ E_{(m+1)L}^- \end{bmatrix} = \mathbf{S}_j \begin{bmatrix} -\frac{S_{12}}{S_{11}} \\ 1 \end{bmatrix} E_{(m+1)L}^-. \quad (57)$$

We can link the electric field to the light flux coming

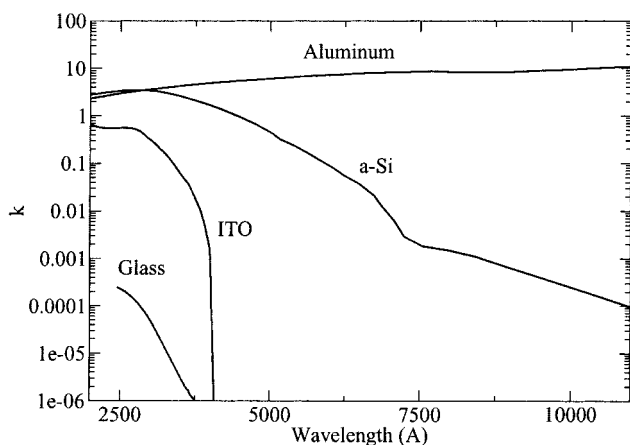


Fig. 6. Extinction coefficient spectra used for the simulations.

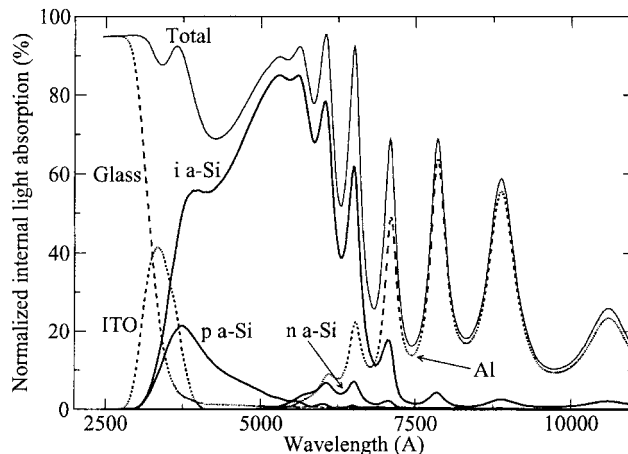


Fig. 7. Calculated normalized internal light absorption at normal incidence for the pin solar cell described in the text. Total absorption ( $100 - R - T$ ) is also shown.

from the right-hand side as follows:

$$\frac{E_{(m+1)L}^-}{E_{0'R}^+} = \left[ \frac{U_{(i'+1)L}^-}{U_{0'R}^+} \right]^{1/2}. \quad (58)$$

From Eqs. (58) and (38) we have

$$E_{(m+1)L}^- = \left\{ (0, 1) \bar{\mathbf{L}}_{i'+1} \bar{\mathbf{S}}_{i'+1} \begin{bmatrix} 1 \\ \bar{\mathbf{S}}_{11} \\ 0 \end{bmatrix} \right\}^{1/2} E_{0'R}^+. \quad (59)$$

By applying again formulas (47)–(56), we can compute the contribution to the energy flux for light coming from the right-hand side,  $\Phi_j^r(x)$ .

Finally, by applying the superposition principle, we have

$$\Phi_j(x) = \Phi_j^l(x) + \Phi_j^r(x). \quad (60)$$

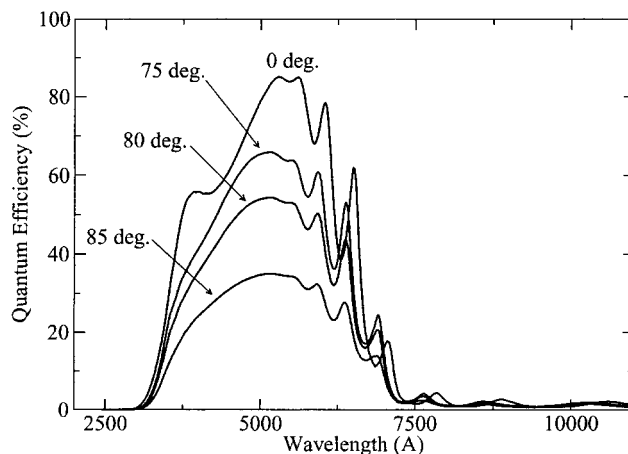


Fig. 8. Calculated quantum efficiencies for different incidence angles.

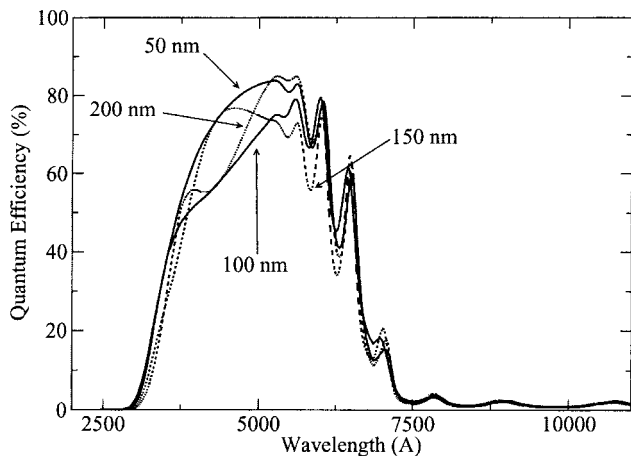


Fig. 9. Calculated quantum efficiencies for different ITO thicknesses.

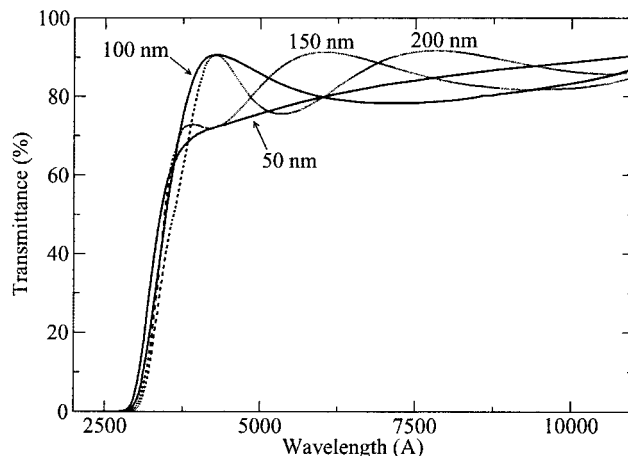


Fig. 10. Calculated transmittance for the structure of ITO on glass (1 mm) for different ITO thicknesses (as in Fig. 9).

### 3. Simulations

The simulations were carried out with a computer code called OPTICAL,<sup>12</sup> developed by the author and based on this work and on a previous code written by C. Summonte, Consiglio Nazionale delle Ricerche, Istituto per la Microelettronica e Microsistemi, Sezione di Bologna, Italy. OPTICAL is open source, multiplatform, and available for free under general public license. As an example of an application I report simulation results on an amorphous-silicon (a-Si) thin-film solar cell. The simulated device has the following structure: Corning glass (1 mm, incoherent)/indium tin oxide (ITO, 200 nm)/*p* a-Si (5 nm)/*i* a-Si (600 nm)/*n* a-Si (50 nm)/Al (500 nm). The indices of refraction used for the simulation are given in Figs. 5 and 6. The light was assumed to be unpolarized. The calculated internal light absorption for each layer normalized to the incident light intensity [obtained with Eq. (2)] is shown in Fig. 7, where we can distinguish the contribution of each layer to the total light absorption of the device, which is computed as  $100 - R - T$ . Light from 250 to 330 nm is almost completely absorbed in the glass (opaque in this region); around 330 nm there is an absorption peak that is due to the ITO; and the absorption spectra of the *p* a-Si layer is centered around 370 nm, of the *i* layer around 520 nm, and of the *n* layer around 620 nm. The main absorption takes place of course in the *i* layer, which is the active region of the device. Interference fringes that are due to multiple reflection in the a-Si layer are visible for wavelengths above 520 nm. Note that above 700 nm (where a-Si becomes transparent) almost all the light is absorbed by the aluminum, with an absorption peak as high as 60%! As expected, the total absorption ( $100 - R - T$ ), which is the experimental quantity we can measure, is equal to the sum of all the internal absorption.

An important characteristic quantity for a solar cell is the quantum efficiency (QE), which is the ratio between collected electrons over incident photons. For a pin solar cell in the first approximation, the collection

probability for a photogenerated electron-hole pair can be considered equal to unity in the *i* layer and zero in all the other layers. Consequently the expected QE of the simulated device can be in the first approximation identified with the internal absorption in the *i* layer. In Fig. 8 the influence of the incidence angle on the QE of the device is reported. We can see that it is for only high-value angles that the effect becomes relevant; the difference is very small below 60°.

In Fig. 9 the effect of ITO thickness on the QE of the device is shown. Interference that is due to ITO thickness strongly affects the QE in the wavelength range from 350 to 600 nm. The best thickness between the tested values seems to be 50 nm. Of course, for device optimization one should consider also the influence that the ITO thickness has on the series resistance of the device.

Note that one cannot simply deduce the best ITO thickness by measuring  $T$  on the substrate before starting the a-Si deposition (a common mistake). This fact is clear in Fig. 10 in which the computed  $T$  for the above situation (ITO on glass) is shown. The transmittance calculated with 50 nm of ITO is actually the lowest one in the range of interest, suggesting the wrong conclusion, i.e., that this thickness should be avoided.

### 4. Conclusion

A method has been presented to compute transmittance, reflectance, and internal light absorption, including the case of oblique incidence, in mixed coherent-incoherent multilayers. The method is based on the calculation of the light energy flux  $\Phi$  inside a multilayer, from which internal light absorption is straightforwardly derived. The Poynting vector is used to derive  $\Phi$  in the case of a coherent layer.

The use of the quantity  $\Phi$  to compute light absorption has several advantages over the more commonly used light intensity  $I$ . For using  $I$ , an integration with a domain discretization is required, which may lead to some errors in the computed data and may require a long computation time. A higher accuracy is

achieved with  $\Phi$  as there is no approximation due to discretization. Moreover, the computer code is simplified and consequently the computation time is much shorter. As an example of an application of the method, a study on a typical a-Si pin solar cell is reported.

## References

1. C. C. Katsidis and D. I. Siapkas, "General transfer-matrix method for optical multilayer systems with coherent, partially coherent, and incoherent interference," *Appl. Opt.* **41**, 3978–3987 (2002).
2. J. S. C. Prentice, "Optical generation rate of electron-hole pairs in multilayer thin-film photovoltaic cells," *J. Phys. D* **32**, 2146–2150 (1999).
3. K. Ohta and H. Ishida, "Matrix formalism for calculation of the light beam intensity in stratified multilayered films, and its use in the analysis of emission spectra," *Appl. Opt.* **29**, 2466–2473 (1990).
4. R. M. Azzam and N. M. Bashara, *Ellipsometry and Polarized Light* (North-Holland, 1977), pp. 332–340.
5. J. S. C. Prentice, "Coherent, partially coherent and incoherent light absorption in thin-film multilayer structures," *J. Phys. D* **33**, 3139–3145 (2000).
6. K. Ohta and H. Ishida, "Matrix formalism for calculation of electric field intensity of light in stratified multilayered films," *Appl. Opt.* **29**, 1952–1959 (1990).
7. L. A. A. Pettersson, L. S. Roman, and O. Inganas, "Modeling photocurrent action spectra of photovoltaic devices based on organic thin films," *J. Appl. Phys.* **86**, 487–496 (1999).
8. H. Hoppe, N. Arnold, N. S. Sariciftci, and D. Meissner, "Modeling the optical absorption within conjugated polymer/fullerene-based bulk-heterojunction organic solar cells," *Sol. Energy Mater. Sol. Cells* **80**, 105–113 (2003).
9. J. A. Stratton, *Electromagnetic Theory* (McGraw-Hill, 1941), Chap. 12.
10. M. Born and E. Wolf, *Principles of Optics* (Pergamon, 1970), pp. 33.
11. E. D. Palik, *Handbook of Optical Constants of Solids* (Academic, 1991), Vol. II, pp. 38–41.
12. E. Centurioni, "A GPL optical simulation program for mixed coherent/incoherent multilayer systems," available at [www.bo.imm.cnr.it/~centurio/optical.html](http://www.bo.imm.cnr.it/~centurio/optical.html).